



Comparison between Alumina Supported Catalytic Precursors and their Application in Thiophene Hydrodesulfurization: $(\text{NH}_4)_4[\text{NiMo}_6\text{O}_{24}\text{H}_6] \cdot 5\text{H}_2\text{O}/\gamma\text{-Al}_2\text{O}_3$ and $\text{NiMoO}_x/\gamma\text{-Al}_2\text{O}_3$ Conventional System.

Journal:	<i>RSC Advances</i>
Manuscript ID	RA-ART-09-2015-017695.R2
Article Type:	Paper
Date Submitted by the Author:	15-Nov-2015
Complete List of Authors:	Ayala-G, Monica; Cinvestav, Chemistry Puello, Esneyder; Universidad del Atlántico, Chemistry González-García, Gerardo; Universty of Guanajuato, Department of Chemistry Quintana, Patricia; Cinvestav-I.P.N. Unidad Merida, Applied Physics Department Diaz-Uribe, Carlos; Universidad del Atlántico, Chemistry
Subject area & keyword:	Heterogeneous < Catalysis

Comparison between Alumina Supported Catalytic Precursors and
their Application in Thiophene Hydrodesulfurization:
 $(\text{NH}_4)_4[\text{NiMo}_6\text{O}_{24}\text{H}_6]\cdot 5\text{H}_2\text{O}/\gamma\text{-Al}_2\text{O}_3$ and $\text{NiMoOx}/\gamma\text{-Al}_2\text{O}_3$ Conventional
System.

Mónica Ayala-G^{1,2}, Esneyder Puello P^{1,4*}, Patricia Quintana², Gerardo González-
García^{2,3}, Carlos Diaz⁴.

¹*Grupo de Investigación en Oxi/Hidrotratamiento Catalítico y Nuevos Materiales,
Programa de Química-Ciencias Básicas Universidad del Atlántico, Barranquilla-Colombia.*

Corresponding Author: Tel 57-5-3599484,*

email:snypollqco@yahoo.com

²*Departamento de Física Aplicada, Laboratorio Nacional de Nano y Biomateriales del
CINVESTAV del IPN unidad Mérida, Antigua Carretera a Progreso Km. 6, CP. 97310
Mérida, Yucatán, México*

³*Departamento de Química, Universidad de Guanajuato, Noria Alta, s/n. Guanajuato, Gto.,
36050 México*

⁴*Grupo de investigación en Fotoquímica y Fotobiología, Programa de
Química-Ciencias Básicas Universidad del Atlántico, Barranquilla-Colombia.*

Keywords: Thiophene hydrodesulfurization, Molybdate, Anderson-type
heteropolyoxomolybdate, phase composition and structure.

Abstract

The effect of the phase composition of alumina supported NiMo catalytic precursors on thiophene hydrodesulfurization (HDS) was investigated. The catalytic precursors were prepared by impregnation of the commercial γ -Al₂O₃ with solutions of Anderson-type ammonium salts or co-precipitation of ammonium heptamolybdate and nickel nitrate. The precursors were characterized by XRD, BET specific surface area, pore volume and pore size, XPS, elemental analysis, TGA and ²⁷Al MAS NMR. The chemical analyses by ICP showed for the NiMo-AP compounds a clear coincidence between experimental and theoretical values according to stoichiometric values (Mo/Ni= 6), while for the NiMo-COP deviations were observed (Mo/Ni~7). The specific surface area and pore volume of NiMo-AP/ γ -Al₂O₃ precursors were greater than those of the NiMo-COP/ γ -Al₂O₃ precursors (387/325 m²/g vs. 283/265 m²/g) and (0.34/0.27 cm³/g vs. 0.21/0.15 cm³/g) respectively; whereas the average pore radius for all systems was 12 Å. XRD and XPS analysis confirmed the presence of (NH₄)₄[NiMo₆O₂₄H₆]•5H₂O and Mo⁵⁺/Mo⁶⁺ for solids obtained by Anderson-type precursors, whereas NiMo-COP/ γ -Al₂O₃ precursors exhibited Mo⁶⁺ from NiMoO₄ and MoO₃. The NiMo precursor obtained from conventional method showed higher amount of sulfur than those synthesized from Anderson-type phase (6.9 to 4.9 wt%), although this does not mean a highly active sample or optimum sulfided active phase. The ²⁷Al solid-state MAS NMR showed higher tetrahedrally coordinated aluminium for the NiMo-COP/ γ -Al₂O₃ catalytic precursors. The catalytic activity was strongly influenced by the type of catalytic precursor and metallic wt%. The activity of catalysts obtained by the sulfided Anderson-type ammonium salts was greater than the sulfided solids

obtained by the conventional method, suggesting that these precursors originate a better active phase with a molar ratio $(\text{Ni} + \text{Mo})/\text{S} = 1.01$ (likely “Ni–Mo–S” species), due to lower losses of the Ni promoter into the alumina support (^{27}Al NMR) and lowest metal-support interaction (TGA). The catalysts obtained the HDS products were butane and *cis*-butene independent of precursor type. Furthermore, the catalysts with 15 wt% Mo were more efficient than those obtained with 8 wt% Mo.

Keywords: Thiophene hydrodesulfurization, Molybdate, Anderson-type heteropolyoxomolybdate, Catalytic precursor.

1. Introduction

During the combustion of sulfur-containing fuels it is produced SO_x , which causes some of the most detrimental effects in the environment [1]. The current generation of hydrodesulfurization catalysts are $\text{Co}(\text{Ni})\text{-Mo}(\text{W})/\text{Al}_2\text{O}_3$ sulfides, although they are very active for conventional oil, these have some limitations such as the difficulty in its sulfurization and the strong interaction between support and active species, which make that exhibit low activity towards highly refractory sulfur compounds [2]. This has led to the governments of numerous countries to adopt new regulations which aim to a significant reduction of sulfur content in fuels (10 ppm or less) [3]. This is a challenging task and it is reported that to bring the sulfur level from presently higher than 500 down to 15 ppm level needs catalysts, which are ~7 times more active than the existing ones [4, 5]. The present HDS catalysts require harsh conditions that result in high operating cost (*e.g.*, high temperature,

high pressure, and high hydrogen consumption) [4]. Therefore, it is highly desired to develop new technologies for raising the catalytic activity, which are based in novel catalyst formulations that can fulfill these environmental regulations, either using carriers with various acidic/base properties modified for additives in the impregnating solution or using new starting materials for the preparation of the impregnating solutions [6].

The most widely used hydrotreating (HDT) support is the alumina, because it has excellent mechanical and dispersion properties [7, 8]. Usually, the active components are loaded on the alumina using cobalt or nickel nitrates and ammonium heptamolybdate solutions (conventional preparation method). Hence, the wet step results calcination in the formation of mixed aluminium–molybdenum and/or aluminium–nickel species (e.g., aluminates), these kinds of compounds are not active for HDT and seem to play a role in the accumulation of crystals during the calcination step [9-11]. Therefore, it is necessary to cover the alumina surface with a MoO_3 monolayer before Co impregnation to avoid their formation [10]. By taking into account of these limitations, recent studies have shown as potential catalysts for such applications the Anderson type polyoxomolybdates [9, 12]. The planar structure of the Anderson type polyoxomolybdates is a relevant factor in the heteropolyanion-support interaction, producing an active surface with an ordered distribution and uniform deposition of the metallic elements, which favors the synergic effect [13, 14]. Moreover, the catalysts prepared in this way exhibit good reducing and sulphidizing properties, which provide an interesting alternative to HDS traditional systems [15].

The Anderson-type heteropolyanions ($[YM_6O_{24}H_x]^{n-}$) possess a heteroatom (Y) in a central octahedral cavity of the crown formed by six edge-sharing octahedral MO_6 (M = Mo or W) [9]. These polyanions become a family for a number of 2+, 3+, 4+, 6+ and 7+ ions as the heteroatom. They are classified into types of A (x = 0) and B (x = 6) by the number of attached protons [16].

In recent years, several studies have presented the use of heteropolyoxomolybdate in the preparation of HDS catalysts [17, 18]. Hence Cabello *et al.*, have showed that Co, Ni or Rh containing heteropolymolybdates with Anderson-type structure supported on $\gamma-Al_2O_3$ are interesting precursors in heterogeneous catalysts for HDT processes. This new system shown that the HDS of thiophene gave a higher activity at a lower Co(Ni)/(Co(Ni)+Mo) molar ratio (0.14), as compared to 0.25–0.40 in the conventional system [15]. Spojakina *et al.* prepared by mechanochemical mixing, TiO_2 -supported Fe, Co, or Ni heteropolymolybdates of Anderson type. The Ni-containing catalyst reveals the highest and the most stable activity comparable with Co and Fe containing catalysts. Their HDS activity is compared to those of alumina and titania catalysts synthesized by the conventional impregnation method [19]. Palcheva *et al.* reported the preparation by impregnation of the supported Anderson-type heteropolyoxomolybdate. The addition of Co, Ni, or B influenced the Al_2O_3 phase composition and gave increased catalytic activity for 1-benzothiophene HDS (the prior loading of Ni, Co or B increased the degree of sulfidation of the catalysts) [20]. Nikulshin *et al.* obtained $XMo_6(S)/Al_2O_3$ and $Ni_3-XMo_6(S)/Al_2O_3$ structures from heteropolycompounds (HPCs) of Anderson type (where X= Co, Ni, Cr, Mn, Fe, Cu, Zn, Ga). The heteroatom plays an important role in the formation and

behavior of the HDT and HDS active sites (the Ni HPCs was the most active). It was found that heteropolycompounds are effective precursors of a multilayered active phase of hydrotreating catalysts [21].

Despite reports in the literature on the synthesis of heterogeneous hydrotreating catalysts from Anderson type heteropolycompounds; less emphasis has been made on the comparison of these catalysts and the conventional ones prepared at the same composition (i.e., with non-optimized Mo/promoter contents), thus it is not yet clear how these systems work in HDS although the Ni content is considerably lower ($[\text{Ni}]/([\text{Ni}]+[\text{Mo}])= 0.14$ in relation to 0.25–0.40 in the conventional system. For this reason, the purpose of this investigation was to provide a comparison of conventional-like NiMo/alumina catalysts with similar composition catalysts prepared from heteropolymolybdate complexes (HPMs) on the HDS Activity, because such study will lead to better understanding of active catalyst structure and HDS performances. ,

2. Experimental

2.1 Preparation of precursors

Two types of catalytic precursors were synthesized with Ni/Mo molar ratio 1:6; one of the precursors was prepared using Anderson ammonium salts and the other by one step co-impregnation (conventional-like NiMo/alumina catalysts) [22-24]. Then, In all the runs, 2 g of commercial $\gamma\text{-Al}_2\text{O}_3$ (YPF Oil Company, 328 m^2/g , 4.6 nm, 0.37 cm^3/g and mesh 100-140) was impregnated in excess of pore volume to provide an uniform coating of the alumina surface. The precursor from heteropolymolybdate complexes was prepared adding dropwise a aqueous

solutions of NiMo-AP (8-15 wt % Mo and 1-3 wt % Ni) to a flask containing the support, under stirring at 323 K and pH around 5-6. The impregnation step lasted until removal of the solvent by evaporation. Finally, the mass obtained was further dried at 423 K for 12 h overnight. The conventional NiMo catalyst was prepared adding dropwise to a flask containing commercial γ -Al₂O₃ suspended in a small amount of water, aqueous solutions of ammonium heptamolybdate (Merck, 99%; 8 and 12 wt% for Mo) and nickel nitrate (Riedel de Haen, typically 98%; 1 and 3 wt % Ni), simultaneously. Then it was warmed up to 353 K and kept under stirring at pH 5-6. The solvent was removed by evaporation and the mass obtained was further dried at 393 K for 12 h overnight. Then, the sample was moved to a tubular furnace and treated with air at a flow rate of 50 cm³/min. calcination of the precursor was carried out at 773 K for 4 h [22].

The alumina supported NiMo precursor were identified as NiMo-TP/ γ -Al₂O₃, where TP is the type of precursor (AP: Anderson phase or COP= conventional oxidic phase).

2.2 Catalyst characterization

The Mo and Ni content was determined by optical emission spectrometers with inductively coupled plasma (ICP plasma) using a PERKIN ELMER Optima 7300DV spectrometer. Scanning electron microscopy (SEM) with EDS analysis was performed by a Microscope Philips XL-30 with dispersive energy system for microanalysis with an EDAX DX-4. Sulfur elemental analysis was carried out by means of a combustion method employing a Fisons EA 1108 CHNS-O analyzer in solids HDS postreaction.

The textural properties were determined by means of the physisorption of N₂ at 77 K using a BELSORP 285A/18SA/18PLUS instrument (BEL Japan Inc.). The surface areas of samples were calculated by the Brunauer–Emmett–Teller multipoint method (BET) and, the micropore volume (V_{mi}) were evaluated by the t-plot method and mesopore volume (V_{me}) was estimated by the Barrett–Joyner–Halenda (BJH) method [25]. The total pore volume was evaluated by summation of microporous and mesoporous volumes. The mean pore diameter, D_p , was calculated from $D_p = 4V_T/S$ [26], where V_T is the total volume of pores, and S being the BET surface area.

XRD analysis of the samples was carried out using a BRUKER D8 ADVANCE diffractometer with a Cu $K\alpha$ radiation source ($\lambda = 1.5418 \text{ \AA}$) and Ni filter, within the range $5^\circ \leq 2\theta \leq 90^\circ$. Identification of the different phases was made using the JCPDS library [27] for (NH₄)₄[NiMo₆O₂₄H₆]•5H₂O (card No. 22-0506), NiMoO₄ (card No. 09-0175), MoO₃ (card No. 01-0706) and γ -Al₂O₃ (card No. 10-0425). The FT-IR spectra were carried out by means of a Nicolet MAGNA-IR 560 spectrometer. The catalyst samples were ground to a very fine powder with KBr and the mixture was pressed into a transparent disk containing ca. 2 wt. % of sample then placed directly in the infrared beam in a suitable holder, in air.

The surface composition of the precursors were determined by means of X-ray photoelectron spectroscopy (XPS) with a ThermoScientific K-Alpha spectrometer, equipped with a dual (non-monochromatic) Mg/Al anode, operated at 400W. The Al $K\alpha$ radiation (1486.6 eV) was employed for the experiments reported here. All measurements were performed under UHV, better than 10^{-9} Torr. Calibration of the instrument was done employing the Au 4f_{7/2} line at 83.9 eV. Quantification of

the XPS signals and curve fitting of the spectra was carried out with the XPSPEAK 4.1 and XPS GRAPH routines after baseline subtraction by the Shirley method, employing typically an 80% Gaussian-20% Lorentzian combination and tabulated atomic sensitivity factors. Due to the relatively insulating character of samples, internal referencing of binding energies was made by using the dominating Al 2p peak of the support at 74,4 eV. Binding energies reported in the current study were accurate to within 0,2 eV.

Solid-state magic-angle spinning (MAS) ^{27}Al NMR was used to study alumina support and the structure of catalysts. Quantitative NMR spectra were recorded at 295 K on a Varian/Agilent Premium Compact 600 NMR spectrometer with rotors of ZrO_2 (diameter 4.2 mm). $\pi/2$ pulse of 2,0 μs and 60,0 s of recycle delay were used. Chemical shifts (ppm) were determined relative to external 1,0 M solution of $\text{Al}(\text{NO}_3)_3$ (0,0 ppm).

The thermal analysis was used to study the thermal stability of oxidic precursors unsupported and supported in function of temperature. TG and DTG measurements were carried out on a TA Instrument model Discovery working in an N_2 stream. The heating rate was $10^\circ\text{C min}^{-1}$ and the temperature was raised up to 900°C .

2.3 Catalytic test

Prior to the catalytic reaction, the catalytic precursors were activated by sulfiding in situ under a 1 vol% CS_2/H_2 mixture at 673 K for 2 h. Tests of thiophene HDS were carried out in a fixed bed, continuous flow reactor, at 673 K and atmospheric pressure. The test conditions were: 250 mg^{-1} of catalyst (mesh 100-120), flow of 100

$\text{cm}^3 \text{min}^{-1}$ of the thiophene (2.27 mol%)/ H_2 mixture. Thiophene consumption during the course of reaction was followed by means of gas chromatography, with sampling of the gaseous effluents of the reactor occurring at 15 min intervals. After stabilization ($\sim 2\text{-}3$ h), the catalytic activities of Ni-Mo catalysts were determined.

Absence of mass and heat flow transport effects was verified according to established procedures [28]. All experiments reported in this work (synthesis protocols, characterizations and catalytic activity measurements) were carried out at least in duplicate. Good reproducibility was verified, better than 10% in all quantitative measurements.

3. Results and Discussion

3.1 Chemical analysis

Results obtained from EDS and ICP chemical analyses are shown in Table 1. The ICP analyses for the supported and unsupported NiMo-AP compounds displayed a clear coincidence between experimental and theoretical values according to the atomic ratio $\text{Mo}/\text{Ni} = 6$, while supported NiMo-COP presented deviations ($\text{Mo}/\text{Ni} \sim 7$). Hence, the proposed formula of those Anderson heteropolyanion deduced from the elemental analysis, is in agreement with that expected, *i.e.*, $(\text{NH}_4)_4[\text{NiMo}_6\text{O}_{24}\text{H}_6] \cdot 5\text{H}_2\text{O}$ has atomic ratio $\text{Mo}/\text{Ni} = 6$. Figure 1 shows the SEM image of the synthesized NiMo systems. According to the micrographs observed, agglomeration of nanoparticles (see below) occurs; with the agglomerate size ranging from 0.5 to 2 μm . Likewise, SEM microscopy revealed laminar morphologies in all NiMo-AP/ $\gamma\text{-Al}_2\text{O}_3$ precursor. The EDS spectra confirmed the presence of the atoms constituting the precursor, *i.e.* Ni, Mo, Al and O.

3.2 The textural properties

The type of precursor prepared differs by their textural characteristics from each other (see Table 1). Both series of catalysts show similar trends, the surface area decreasing for samples containing Mo and Ni respect the bare support (except for NiMo-AP(8 wt%)/ γ -Al₂O₃), which is in line with the fact that NiMo oxides tend to cover the surfaces of supports and thus block micro- and mesoporous. The precursors of NiMo-AP/ γ -Al₂O₃ showed higher values of surface area (387 and 325 m²/g), pore volume (0.419 and 0.343 cm³/g) and pore size (4.3 and 4.2 nm) than the NiMo-COP/ γ -Al₂O₃ precursors (283-265 m²/g, 0.277-0.220 cm³/g and 3.8-3.3 nm, respectively). This behavior can be related with the migration of the metallic phase into the support pores decreasing their pore volume (V_{mes}/V_T) and therefore its surface area [29]. The pores for the present precursors mostly locate in the range of mesoporous (2-50 nm), however the pore size distribution have a peak near 1.2 nm (microporous, not shown here).

3.3 XRD analysis

The XRD patterns of catalysts varying the according to the catalytic precursor (Figure 2 and 3). The XRD patterns depending of the wt% Mo and type of precursor. The NiMo-AP(15)/ γ -Al₂O₃ showed diffraction peaks corresponding to (NH₄)₄[NiMo₆O₂₄H₆]•5H₂O at $2\theta = 17.39, 15.30, 11.05, 29.48, 28.52, 12.31, 34.09, 23.79, 16.39$ and γ -Al₂O₃ at $2\theta = 67.10, 45.90, \text{ and } 37.64$ (only 29.48 and 28.52 to NiMo-AP(8)/ γ -Al₂O₃); while NiMo-COP(15)/ γ -Al₂O₃ precursor displayed NiMoO₄ at $2\theta = 29.09, 32.81, 25.60, 43.95, 47.61, 41.22, 14.47$; MoO₃ at $2\theta = 27.44$ and γ -

Al_2O_3 at $2\theta = 67.10, 45.90,$ and 37.64 (NiMo-COP(8)/ $\gamma\text{-Al}_2\text{O}_3$ no signals were observed). The peaks corresponding to NiMo precursors (15 wt% Mo) clearly appear in the XRD of supported catalysts, so that the skeletal structure of Anderson phase or $\text{NiMoO}_4/\text{MoO}_3$ is certainly retained upon adsorption on support. Thus, intense and defined diffraction peaks were observed in the XRD spectra (Figure 2), which suggest that these NiMo-AP/ $\gamma\text{-Al}_2\text{O}_3$ phases have better crystallinity than those of conventionally synthesized samples (Figure. 3). Also by comparing the XRD spectra in Figures 2 and 3, it can be seen that the reflection peaks disappear when the phase was 8 wt% Mo that those of 15 wt%, it is probably because the crystallites are too small to give XRD signals or the particles of NiMo were well dispersed on the support.

3.4 FTIR analysis

The FT-IR vibrational spectra for all precursors in $4000\text{--}400\text{ cm}^{-1}$ range, is presented in Figures 4 and 5 Indifferently from the used precursor type, the bands appearing at approximately in regions between $3600\text{--}2800, 1700\text{--}1400, 1000\text{--}850, 750\text{--}550$ and $< 450\text{ cm}^{-1}$ that can be assigned to the characteristic vibrations of O–H and/or N–H stretchings, O–H and N–H bendings, Mo–O₂ terminal stretchings, Mo–O–Mo bridge stretchings and Ni–O respectively [14, 30]. However, the type of precursor, bands intensity and shape depend on the precursor. Additionally, it can be seen that vibration bands intensity corresponding to unsupported samples are higher than those supported due to the low content of active phase caused by its dilution or anchoring on the $\gamma\text{-Al}_2\text{O}_3$ matrix. The absence of prominent shifts in the position of these peaks, relative to the bulk NiMo

species, suggests that the structure is retained after immobilization on the surface of $\gamma\text{-Al}_2\text{O}_3$.

3.5 XPS analysis

The XPS spectra for the NiMo/ $\gamma\text{-Al}_2\text{O}_3$ catalysts (Figure 6 and 7) show Mo $3d_{5/2-3/2}$ and Ni $2p_{3/2-1/2}$ regions, which are typical of those obtained with the rest of Mo and Ni-containing catalysts. The Mo $3d_{5/2}$ signals suggest the presence of Mo $^{5+}$ (230.9 eV) and Mo $^{6+}$ (232.5 eV) species on the surface of NiMo-AP/ $\gamma\text{-Al}_2\text{O}_3$, whereas NiMo-COP/ $\gamma\text{-Al}_2\text{O}_3$ showed the presence at the surface of Mo $^{6+}$, these values agree with the reported values [31-33]. The use of NiMo-AP precursors, indifferently from the wt% Mo (shown here the 15 wt%), generated species of Mo $^{5+}$ possibly by redox properties in the heteropolyanion planar structure associated to iso- and heteropolymolybdates (and -tungstates) are easily reducible and generate the partially reduced compounds (it is interesting for major sulfiding). Whereas, the NiMo-COP precursor generated only Mo $^{6+}$ species as it usually occurs in the conventional procedure (Table 2 for atomic %). The Ni 2p spectrum shows a Ni $2p_{3/2}$ peak at 856,5 eV with a strong shake-up line at 862.0 eV (Figure 7). These signals suggest the presence of Ni $^{2+}$ species, which may be either NiMoO $_4$ or NiAl $_2$ O $_4$ [34].

The amount of nickel and molybdenum at the surface (atomic % XPS) obtained by conventional method at 15 wt% Mo is consistently higher than the Anderson phase, it is possibly due to either aggregation or "stacking" of Mo and Ni during the synthesis (co-precipitation on the external surface of alumina powder), while in NiMo-AP/ $\gamma\text{-Al}_2\text{O}_3$ synthesis the heteropolyanion planar structure exhibits uniformity

in the deposition (see, Ni/Al and Mo/Al in Table 2) as it has been reported by Cabello *et al.* [9, 15], hence the Ni/Mo atomic ratios (by XPS) were in agreement with ICP analysis for the stoichiometric catalysts. The slight difference in the atomic % for NiMo-COP/ γ -Al₂O₃ may be related to an irregular distribution of the various phases on the surface of this solid (blocking of the support pores volume, Table 2).

3.6 ²⁷Al NMR analysis

The information on the relative occupancy of tetrahedral and octahedral aluminium sites in alumina was obtained using ²⁷Al solid-state MAS NMR. Figure 8 shows for NiMo/ γ -Al₂O₃ catalysts the typical ²⁷Al NMR spectra with chemical shift ranges for octahedrally coordinated aluminium (AlO₆) at 9.8 ppm and 67.0 for tetrahedrally coordinated aluminium (AlO₄) and the octahedral:tetrahedral aluminum ratio varies depending on the type of precursor. The peaks related to the AlO₆ units are narrow and symmetric, whereas the peaks related to the AlO₄ resulted broad [35]. By integrating the peak areas, the ²⁷Al octahedral/tetrahedral ratio was 4.62 and 3.37 in NiMo-AP/ γ -Al₂O₃ and NiMo-COP/ γ -Al₂O₃, respectively. The AlO₄ content in the oxidic precursor obtained by conventional method was greater than that of the solids obtained by the Anderson-type ammonium salts, suggesting the existence of aluminates.

3.7 Catalytic test

Thiophene HDS activities are reported as pseudo-first-order rate constants for thiophene disappearance in units of moles of thiophene converted to products per gram of catalyst per minute (mol Th/g cat min) after ~2-3 h of reaction time (steady

state). The samples were presulfided before the activity tests in order to attain a reproducible and stable initial state of the catalytic surface. The catalysts obtained showed no correlation between HDS activity and surface area. The Figure 9 and Table 2 shows that the catalytic activity of catalysts was strongly influenced by the type of catalytic precursor and metal wt%, hence the HDS activity obtained by the sulfided $(\text{NH}_4)_4[\text{NiMo}_6\text{O}_{24}\text{H}_6]\cdot 5\text{H}_2\text{O}/\gamma\text{-Al}_2\text{O}_3$ were greater than those obtained by the conventional method, independently of the Mo and Ni contents. The overall rate of the thiophene HDS (sulfided precursors) was found to increase as follows: NiMo-AP < NiMo-COP(8 wt% Mo)/ $\gamma\text{-Al}_2\text{O}_3$ < NiMo-AP(8 wt% Mo)/ $\gamma\text{-Al}_2\text{O}_3$ < NiMo-COP(15 wt% Mo)/ $\gamma\text{-Al}_2\text{O}_3$ < NiMo-AP(15 wt% Mo)/ $\gamma\text{-Al}_2\text{O}_3$; whose the deactivation behavior is more pronounced for conventional catalytic precursors (see Fig 10).

Table 1 show that the amounts of sulfur and carbon (coking), after of HDS reaction are two times higher in the catalytic precursors obtained by conventional method than those synthesized from Anderson-type phase. This can be expected due to the large amount of metal on the surface (XPS analysis). However, the amounts of sulfur measured by the combustion technique are lower than needed to fully sulfide Mo to MoS_2 and Ni to NiS. Using the nominal compositions, the 15 wt% Mo catalysts would require about 11 wt% S, while the 8 wt% Mo ones need about 5.7 wt% S. Also, the unsupported Anderson-type precursor, if fully sulfided, would require up to 18.7 wt% S, while the results show only 7.56 wt% S in this case. The latter result suggests that the sulfiding conditions do not produce the total sulfuration, However NiMo-AP(15 wt% Mo)/ $\gamma\text{-Al}_2\text{O}_3$ has a molar ratio $(\text{Ni} + \text{Mo})/\text{S} = 1.01$ that allows assume the formation of optimal "Ni-Mo-S" species involved in the catalytic activity of hydrodesulfurization reactions instead of assuming that is not

completely sulfiding the oxidic phase [36]. Likewise, the increase of the activity could be associated to an effective coverage on support surface, suggesting that the Anderson type heteropolyanion has advantages in relation to the conventional procedure in regard to the planar structure of the heteropolyanion (D3d planar symmetry), which ensures an adequate dispersion of the metallic sites achieving a good contact with the support surface and less interaction metal-support as shown TGA (see Fig 11, total weight loss of ~18 %), whereas the precursors NiMo-COP/ γ -Al₂O₃ lose less weight (~10 %), due to the strong interaction (see tables 1 and 2, ρ and V_p against metallic content measured by XPS).

It is well known that the HDS of thiophene on sulfided alumina-supported NiMo oxides leads to butane, *trans*-butene, 1-butene, *cis*-butene and 1,3-butadiene. The catalysts obtained independently of precursor type produced butane and *cis*-butene in the HDS reaction (Table 3). Thus, sulfur removal without hydrogenation of olefins is significant as it has been reported by Pawelec *et al* [37]. The catalysts with 15 wt% Mo and 1.5 wt% Ni were more efficient to butane and *cis*-butene than those obtained with 8 wt% Mo, suggesting that the surface species amount are important for the HDS reactions.

Conclusions

The comparison of conventional-like NiMo/alumina catalysts with similar composition catalysts prepared from heteropolymolybdate complexes (HPMs) on the HDS Activity was provided. For this reason, the influence of the type of catalytic precursor on the thiophene hydrodesulfurization was determined by XRD, textural properties, XPS, ICP, EDAX, TGA, XRD and ²⁷Al NMR. The chemical analyses by

ICP for the NiMo-AP showed stoichiometric values Mo/Ni= 6 and NiMo-COP exhibited an atomic ratio of 7, while EDS spectra confirmed the presence of Ni, Mo, Al and O. SEM microscopy revealed laminar morphologies in all NiMo-AP/ γ -Al₂O₃ precursors with the agglomerate size ranging from 0.5 to 2 μ m. The specific surface area and pore volume of NiMo-AP/ γ -Al₂O₃ precursors were greater than NiMo-COP/ γ -Al₂O₃, although pore diameter for all precursors was 1.2 nm. XRD confirmed the presence of (NH₄)₄[NiMo₆O₂₄H₆]•5H₂O for solids obtained by Anderson-type ammonium salts and a mixture of NiMoO₄ and MoO₃ for precursors obtained by NiMo-COP. The XPS analysis showed two types of molybdenum assignable to Mo⁵⁺ and Mo⁶⁺ on the surface of NiMo-AP/ γ -Al₂O₃ and Mo⁶⁺ at the surface of NiMo-COP/ γ -Al₂O₃, whose abundance was influenced by the precursor type and wt% Mo and Ni. The ²⁷Al-NMR octahedral/tetrahedral ratio was 4.62 and 3.37 in NiMo-AP/ γ -Al₂O₃ and NiMo-COP/ γ -Al₂O₃, respectively. The catalytic activity of oxidic precursor was strongly influenced by the type of precursor and wt% metallic. In consequence, the activity of precursors obtained by the Anderson-type ammonium salts was greater than that of the solids obtained by the conventional method. Likewise, this increase of the activity could be associated to an effective coverage on support surface and less interaction metal-support as shown TGA (it loses less weight due to the strong interaction). The NiMo-AP (15 wt% Mo)/ γ -Al₂O₃ was the precursor most active and it had a molar ratio (Ni + Mo)/S = 1.01 that allows assume the formation of "NiMoS" optimal species involved in the HDS. The catalysts obtained independent of precursor type the HDS products were butane and cis-butene. In the present work it is shown that the use of NiMo Anderson-type

precursors provides better dispersion metallic sites, which are then activated by sulfidation increasing the effectiveness of such catalyst for HDS compared with the catalysts prepared by the traditional method.

Acknowledgments

Laboratorio Nacional de Nano y Biomateriales (LANNBIO), CINVESTAV-IPN Mérida by the projects FOMIX-Yucatán 2008-108160 and CONACYT Lab-2009-01 No 123913. The authors are particularly grateful to Ana R. Cristobal for (SEM-EDS), Liz Cubillaw (FTIR, IVIC), E. Severino (CHNOS, IVIC) and Eduardo Rada (ICP, Quintal-Col.) for their technical assistance. E.P.P dedicated to Ofelia Polo (R.I.P.) and the GIOHCUA research. GGG thanks to CONACYT for Postdoctoral Scholarship at CINVESTAV-IPN Mérida.

References

1. I.V. Babich, J.A. Molijn. Science and technology of novel processes for deep desulfurization of oil refinery streams: a review. *Fuel* 82 (2003) 607.
2. C.C. Yu, S. Ramanathan, B. Dhandapani, J.G. Chen, S.T. Oyama. Bimetallic Nb-Mo Hydroprocessing Catalysts: Synthesis, Characterization and Activity Studies. *J. Phys. Chem. B* 101 (1997) 512.
3. F. Lin, Y. Zhang, L. Wang, Y. Zhang, D. Wang, M. Yang, J. Yang, B. Zhang, Z. Jiang, C. Li. Highly efficient photocatalytic oxidation of sulfur containing organic compounds and dyes on TiO₂ with dual cocatalysts Pt and RuO₂. *Appl. Catal. B* 127 (2012) 363–370.
4. C. Song. An overview of new approaches to deep desulfurization for ultra-clean gasoline, diesel fuel and jet fuel. *Cat. Today*, 86 (2003) 211–263
5. H. Topsøe, B.S. Clausen, F. E. Massoth. Hydrotreating catalysis science and technology. In: Anderson JR, Boudart M, editors. *Catalysis –science and technology*, vol. 11. Berlin, Heidelberg, New York: Springer-Verlag; 1996. p.310.
6. P. A. Nikulshin, A. V. Mozhaev, A. A. Pimerzin, V.V. Konovalov, A. A. Pimerzin. CoMo/Al₂O₃ catalysts prepared on the basis of Co₂Mo₁₀-

- heteropolyacid and cobalt citrate: Effect of Co/Mo ratio. *Fuel* 100 (2012) 24–33.
7. I. Chorkendorff, J. W. Niemantsverdriet. *Concept of Modern Catalysis and Kinetics*. Weinheim: Wiley-VCH Verlag, 2007. 359
 8. R. Chianelli. *Fundamental Studies of Transition Metal Sulfide Hydrodesulfurization Catalysts*. *Catal. Rev. Sci. Eng.* 26 (1984) 361-393.
 9. C.I. Cabello, I.L. Botto, H.J. Thomas. Anderson type heteropolyoxomolybdates in catalysis: 1. $(\text{NH}_4)_3[\text{CoMo}_6\text{O}_{24}\text{H}_6]\cdot 7\text{H}_2\text{O}/\gamma\text{-Al}_2\text{O}_3$ as alternative of Co-Mo/ $\gamma\text{-Al}_2\text{O}_3$ hydrotreating catalysts. *Appl. Catal. A* 197 (2000) 79.
 10. M.H. Pinzón, A. Centeno, S. A. Giraldo. Role of Pt in high performance Pt-Mo catalysts for hydrotreatment reactions. *Appl. Catal. A* 302 (2006) 118–126
 11. P D. Debeckera, M. Stoyanovab, U. Rodemerckb, E. M. Gaigneauxa. Preparation of $\text{MoO}_3/\text{SiO}_2\text{-Al}_2\text{O}_3$ metathesis catalysts via wet impregnation with different Mo precursors. *J. Mol. Catal. A* 340 (2011) 65–76
 12. C. I. Cabello, M. Muñoz, I. L. Botto and E. Payen. The role of Rh on a substituted Al Anderson heteropolymolybdate: Thermal and hydrotreating catalytic behavior. *Thermochimica Acta* 447 (2006) 22–29.
 13. Van Veen JAR, Hendriks PAJM, Andrea RR, Romers EJGM, Wilson AE. Chemistry of phosphomolybdate adsorption on alumina surfaces. 1. The molybdate/alumina system. *J Phys Chem* 1990;94:5275–82.
 14. Pavel A. Nikulshin, Alexander V. Mozhaev, Aleksey A. Pimerzin, Victor V. Konovalov, Andrey A. Pimerzin. CoMo/Al₂O₃ catalysts prepared on the basis of Co₂Mo₁₀-heteropolyacid and cobalt citrate: Effect of Co/Mo ratio. *Fuel* 100 (2012) 24–33.
 15. C. I. Cabello, F. M. Cabrerizo, A. Alvarez, H. J. Thomas. Decamolybdodicobaltate(III) heteropolyanion: structural, spectroscopical, thermal and hydrotreating catalytic properties. *J. Mol. Catal. A* 186 (2002) 89–100
 16. K. Nomiya, T. Takahashi, T. Shirai, M. Miwa. Anderson-type heteropolyanions of molybdenum(VI) and tungsten(VI). *Polyhedron* 6 (1987) 213–218.
 17. A. Spozhakina, N. Kostova, I. Yuchnovski, D. Shopov, T. Yurieva, T. Shokhireva. Synthesis of molybdenum/silica and cobalt—molybdenum/silica catalysts and their catalytic activity in the hydrodesulfurization of thiophene. *Appl. Catal.* 39 (1988) 333-342.
 18. A. Griboval, P. Blanchard, L. Gengembre, E. Payen, M. Fournier, L. Dubois, J.R. Bernard. Hydrotreatment Catalysts Prepared with Heteropolycompound: Characterisation of the Oxidic. *J. Catal.* 188 (1999) 102-110.

19. A. A. Spojakina, E. Y. Kraveva, and K. Jiratova. Heteroatom effect on hydrodesulphurization activity of TiO₂-supported molybdenum heteropolyoxometalates of Anderson type. *Kinet. Catal.* 51(3) (2010) 385–393.
20. R. Palcheva, L. Kaluža, A. Spojakina, K. Jirátová, G. Tyuliev. NiMo/γ-Al₂O₃ Catalysts from Ni Heteropolyoxomolybdate and Effect of Alumina Modification by B, Co, or Ni. *Chin. J. Catal.* 33 (2012) 952–961.
21. P. A. Nikulshin, N. N. Tomina, A. A. Pimerzin, A. Y. Stakheev, I. S. Mashkovsky, V. M. Kogan. Effect of the second metal of Anderson type heteropolycompounds on hydrogenation and hydrodesulphurization properties of XMo₆(S)/Al₂O₃ and Ni₃-XMo₆(S)/Al₂O₃ catalysts. *Appl Catal A* 393 (2011) 146-152.
22. Z. Sarbak. Characterisation of thermal properties of oxide, reduced and sulphided forms of alumina supported Co(Ni)–Mo(W) catalysts prepared by co-precipitation. *Thermochimica Acta* 379 (2001) 1-5.
23. I.L. Botto, A.C. Garcia, H.J. Thomas. Spectroscopical approach to some heteropolymolybdates with the anderson structure. *J. Phys. Chem. Solids* 53 (8) (1992) 1075.
24. C. Martin, C. Lamonier, M. Fournier, O. Mentr'è, V. Harl'è, D. Guillaume, E. Payen. Preparation and Characterization of 6-Molybdocobaltate and 6-Molybdoaluminate Cobalt Salts. Evidence of a New Heteropolymolybdate Structure. *Inorg. Chem.* 43 (2004) 4636.
25. M.A. Díaz-Díez, V. Gómez-Serrano, C. Fernández Gonza'lez, E.M. Cuerda-Correa, A. Macías-García. Porous texture of activated carbons prepared by phosphoric acid activation of woods. *Applied Surface Science* 238 (2004) 309-313.
26. E.P. Barret, P.B. Joyner, P. Halenda, *Journal of the American Chemical Society. The Determination of Pore Volume and Area Distributions in Porous Substances. I. Computations from Nitrogen Isotherms.* 73 (1951) 373-380.
27. Power Diffraction File, ICDD, Newtown Square, Philadelphia, 1995.
28. G.F. Froment, K.B. Bischoff. *Chemical Reactor Analysis and Design.* Willey, 1990.
29. A. Sampieri, S. Pronier, S. Brunet, X. Carrier, C. Louis, J. Blanchard, K. Fajerweg, M. Breyse. Formation of heteropolymolybdates during the preparation of Mo and NiMo HDS catalysts supported on SBA-15: Influence on the dispersion of the active phase and on the HDS activity. *Microporous and Mesoporous Materials* 130 (2010) 130–141.
30. P. A. Nikul'shin, Yu. V. Eremina, N. N. Tomina, and A. A. Pimerzin. Influence of nature of precursors of aluminum-nickel-molybdenum catalysts on their performance in hydrodesulfurization. *Petrol. Chem.* 46(5) (2006) 343–348.

31. Hongying Lü, Wanzhong Ren, Weiping Liao, Wei Chen, Yang Li, Zhanghuai Suo. Aerobic oxidative desulfurization of model diesel using a B-type Anderson catalyst $[(C_{18}H_{37})_2N(CH_3)_2]_3Co(OH)_6Mo_6O_{18} \cdot 3H_2O$. *Appl. Catal. B* 138–139 (2013) 79– 83.
32. C. D. Wagner, W. M. Riggs, L. E. Davis, J. F. Moulder, G. E. Muilenberg, *Handbook of X-Ray Photoelectron Spectroscopy*, Perkin-Elmer, Eden Prairie, Minnesota, 1979.
33. K. Hada, M. Nagai and S. Omi. XPS and TPR Studies of Nitrided Molybdena-Alumina. *J. Phys. Chem. B* 104 (2000) 2090-2098
34. X. Wang, U.S. Ozkan. Characterization of Active Sites over Reduced Ni–Mo/ Al_2O_3 Catalysts for Hydrogenation of Linear Aldehydes. *J. Phys. Chem. B* 109 (2005) 1882–1890.
35. A. Malki, Z. Mekhalif, S. Detriche, G. Fonder, A. Boumaza, A. Djelloul. Calcination products of gibbsite studied by X-ray diffraction, XPS and solid-state NMR. *J. Solid State Chem.* 215 (2014) 8–15.
36. A.S. Walton, J.V. Lauritsen, H. Topsøe, F. Besenbacher. MoS_2 nanoparticle morphologies in hydrodesulfurization catalysis studied by scanning tunneling microscopy. *Journal of Catalysis* 308 (2013) 306–318.
37. B. Pawelec, R. Mariscal, R.M. Navarro, J.M. Campos-Martin, J.L.G. Fierro. Simultaneous 1-pentene hydroisomerisation and thiophene hydrodesulphurisation over sulphided Ni/FAU and Ni/ZSM-5 catalysts. *Appl.Catal., A: Gen.* 262 (2004) 155–166.

Table captions

Table 1. Composition and textural properties in alumina supported Ni-Mo catalyst varying the type of precursor.

Table 2. Distribution of Mo and Ni oxidation states in alumina supported Ni-Mo catalyst using X-ray photoelectron spectroscopy and thiophene hydrodesulfurization activity.

Table 3. Thiophene hydrodesulfurization conversion and selectivity at steady state of sulfided alumina-supported NiMo oxides: effect of wt % and precursor type.

Figure captions

Figure 1. SEM-EDS image of catalytic precursors. (a) NiMo-AP(15 wt% Mo)/ γ - Al_2O_3 and (b) NiMo-COP(15 wt% Mo)/ γ - Al_2O_3 .

Figure 2. X-ray diffraction patterns of NiMo/ γ -Al₂O₃ varying wt% Mo and Ni. (a) NiMo-AP; (b) NiMo-AP(8 wt% Mo)/ γ -Al₂O₃; (c) NiMo-AP(15 wt% Mo)/ γ -Al₂O₃. (*) (NH₄)₄[NiMo₆O₂₄H₆]•5H₂O and (•) γ -Al₂O₃

Figure 3. X-ray diffraction patterns of NiMo/ γ -Al₂O₃ varying wt% Mo and Ni. (a) NiMo-COP(8 wt% Mo)/ γ -Al₂O₃; (b) NiMo-COP(15 wt% Mo)/ γ -Al₂O₃. (*) NiMoO₄, (•) γ -Al₂O₃ and (+) MoO₃.

Figure 4. FT-IR vibrational spectra of NiMo varying wt% Mo and Ni. (a) NiMo-AP; (b) NiMo-AP(8 wt% Mo)/ γ -Al₂O₃; (c) NiMo-AP(15 wt% Mo)/ γ -Al₂O₃.

Figure 5. FT-IR vibrational spectra of NiMo varying wt% Mo and Ni. (a) NiMo-COP; (b) NiMo-COP(8 wt% Mo)/ γ -Al₂O₃; (c) NiMo-COP(15 wt% Mo)/ γ -Al₂O₃.

Figure 6. X-ray photoelectron spectra Mo 3d region of NiMo/ γ -Al₂O₃ varying wt% Mo and Ni. (a) NiMo-COP(15 wt% Mo)/ γ -Al₂O₃; (b) NiMo-AP(15 wt% Mo)/ γ -Al₂O₃.

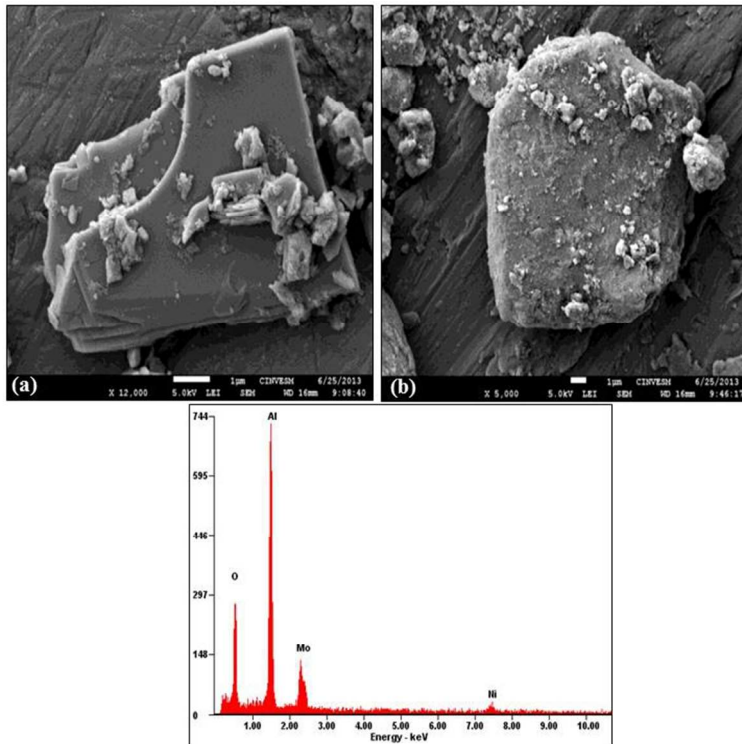
Figure 7. X-ray photoelectron spectra Ni 2p region of NiMo/ γ -Al₂O₃ varying wt% Mo and Ni. (a) NiMo-AP(15 wt% Mo)/ γ -Al₂O₃; (b) NiMo-COP(15 wt% Mo)/ γ -Al₂O₃.

Figure 8. ²⁷Al NMR spectra of NiMo/ γ -Al₂O₃. (a) NiMo-AP(15 wt% Mo)/ γ -Al₂O₃; (b) NiMo-COP(15 wt% Mo)/ γ -Al₂O₃. (*) indicate spinning side bands at 9 KHz.

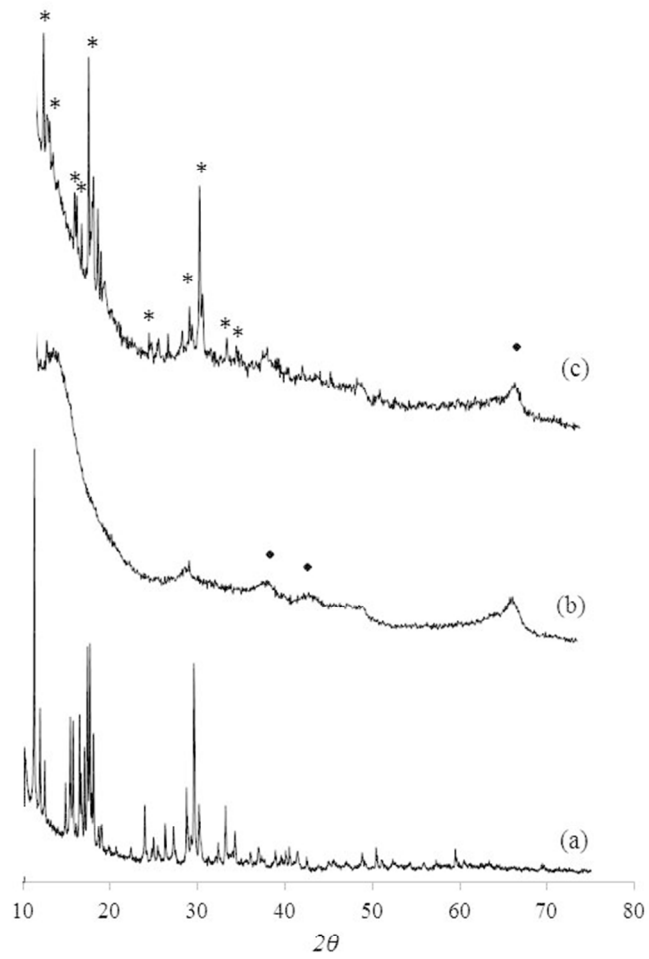
Figure 9. HDS activity at steady state of NiMo-TP/ γ -Al₂O₃ varying metallic wt% and precursor type.

Figure 10. HDS Conversion (%) of NiMo-TP/ γ -Al₂O₃ varying metallic wt% and precursor type.

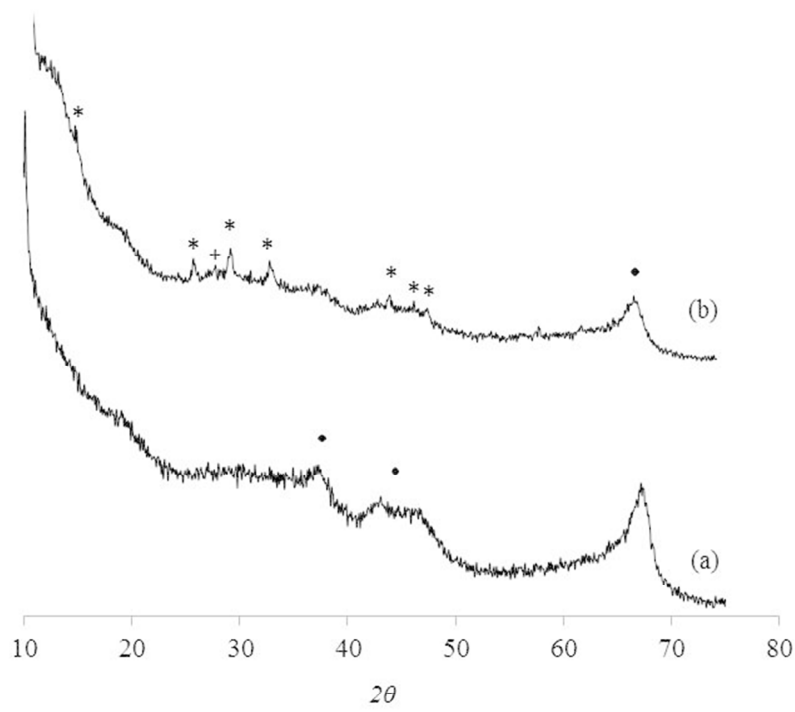
Figure 11. TGA curves of NiMo-COP(15 wt% Mo)/ γ -Al₂O₃, NiMo-AP(15 wt% Mo)/ γ -Al₂O₃ and NiMo-AP.



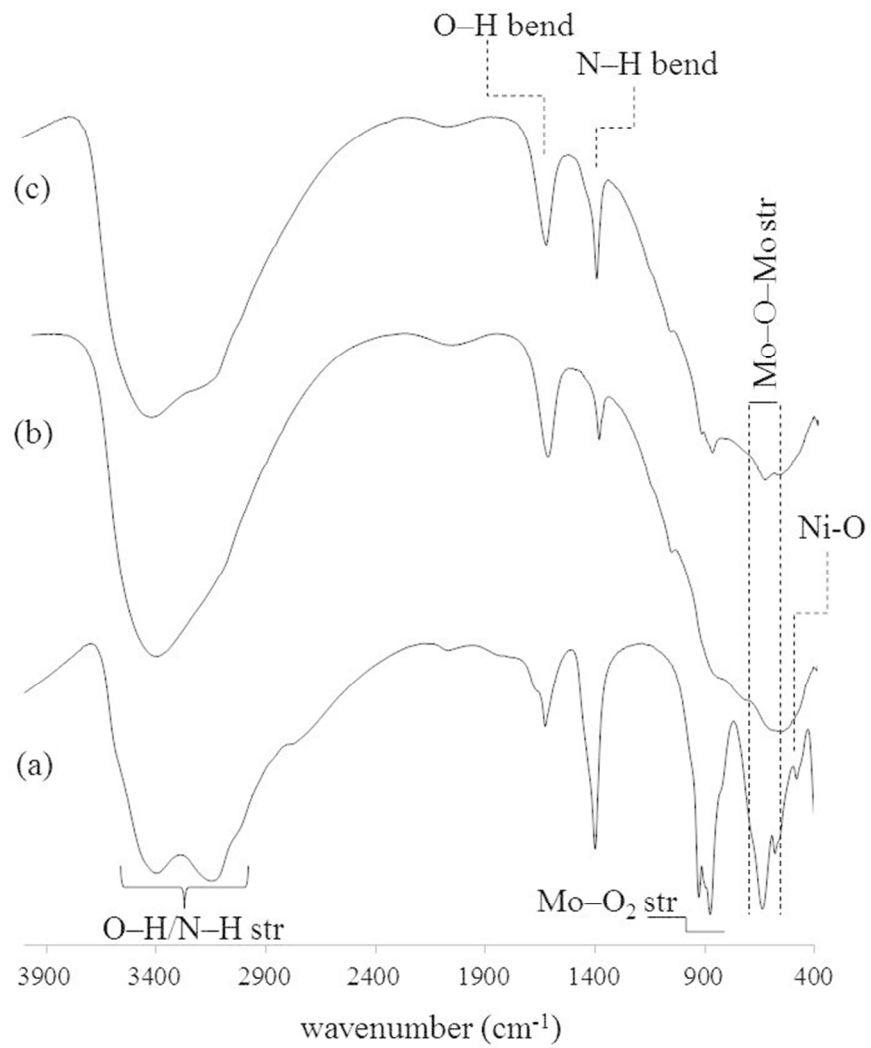
254x190mm (96 x 96 DPI)



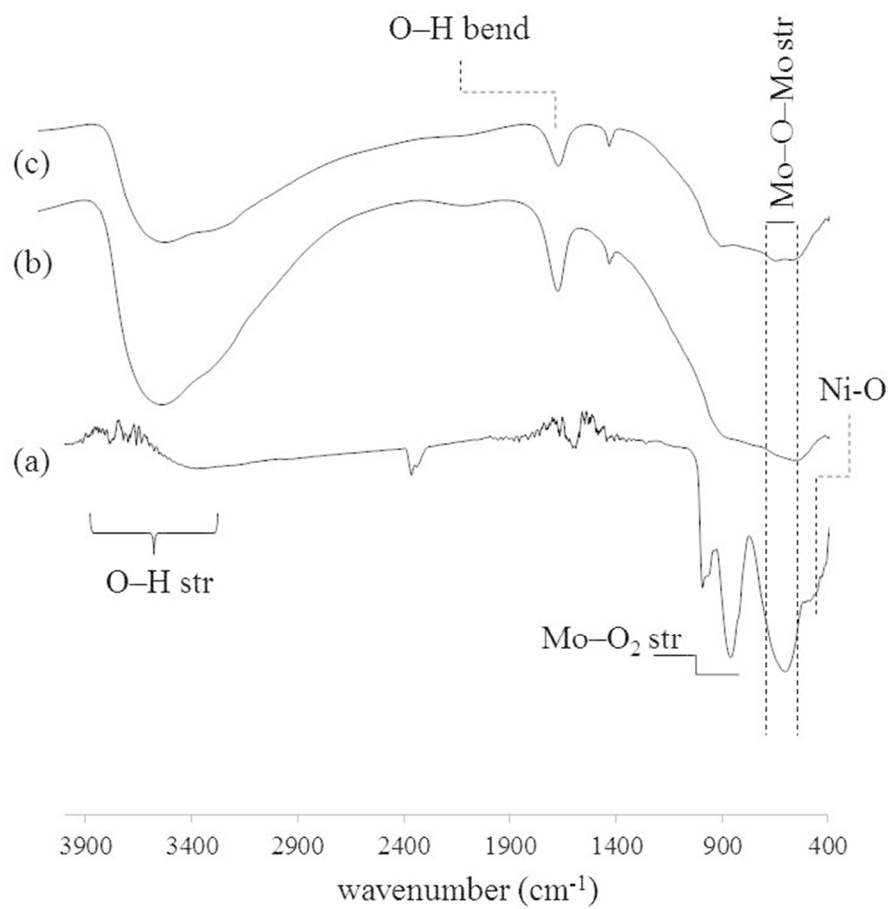
190x254mm (96 x 96 DPI)



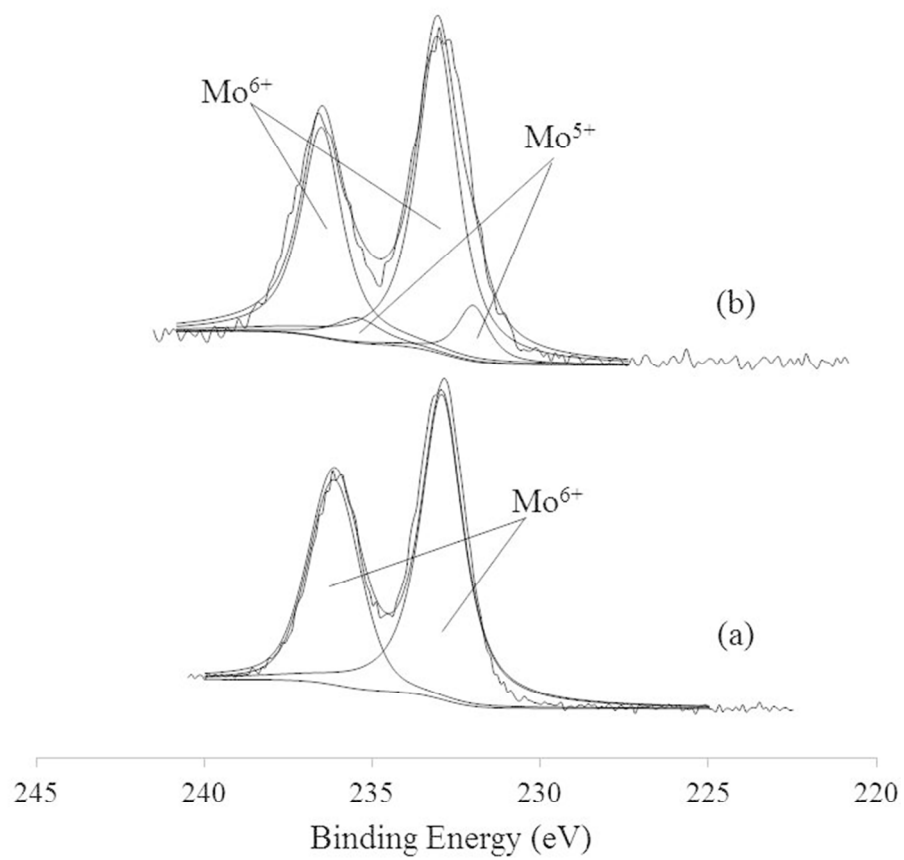
190x254mm (96 x 96 DPI)



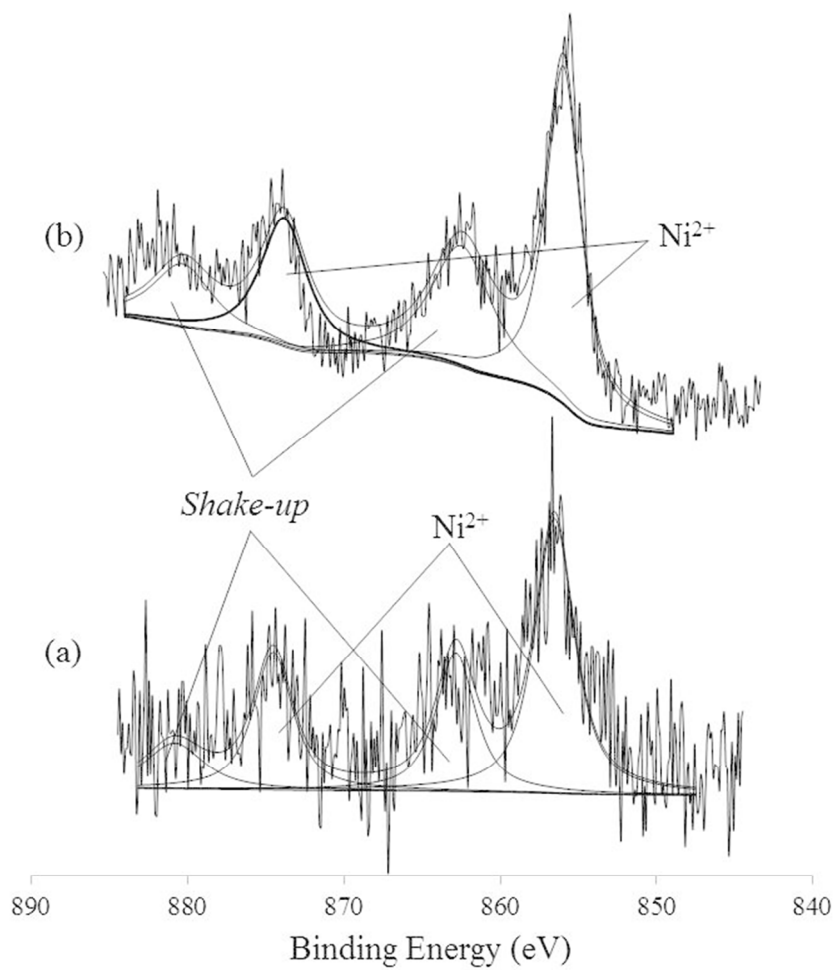
190x254mm (96 x 96 DPI)



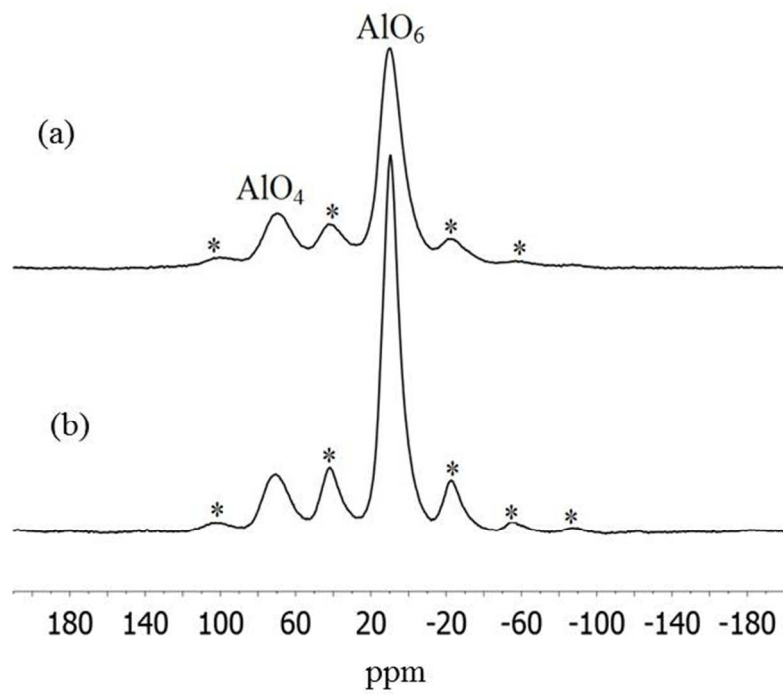
190x254mm (96 x 96 DPI)



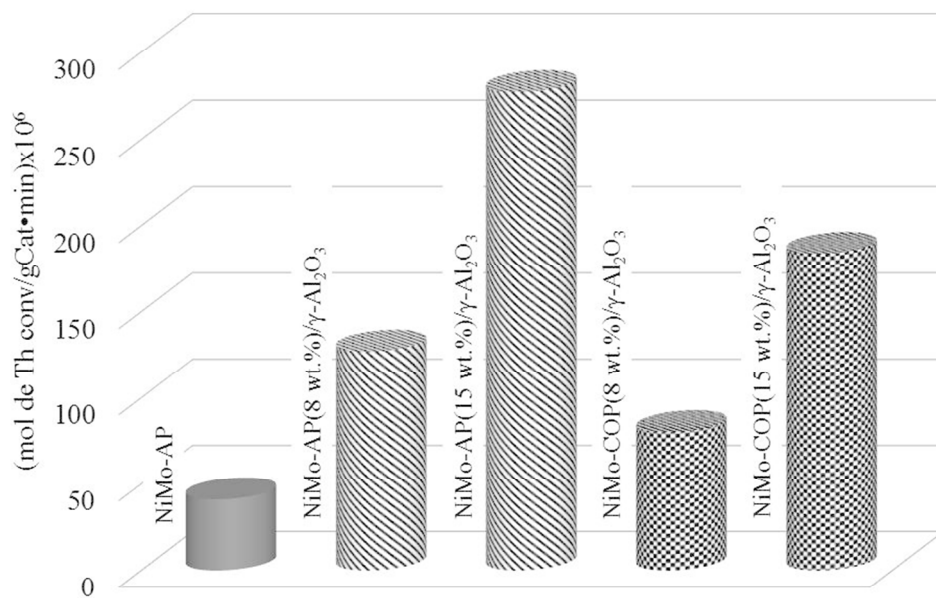
190x254mm (96 x 96 DPI)



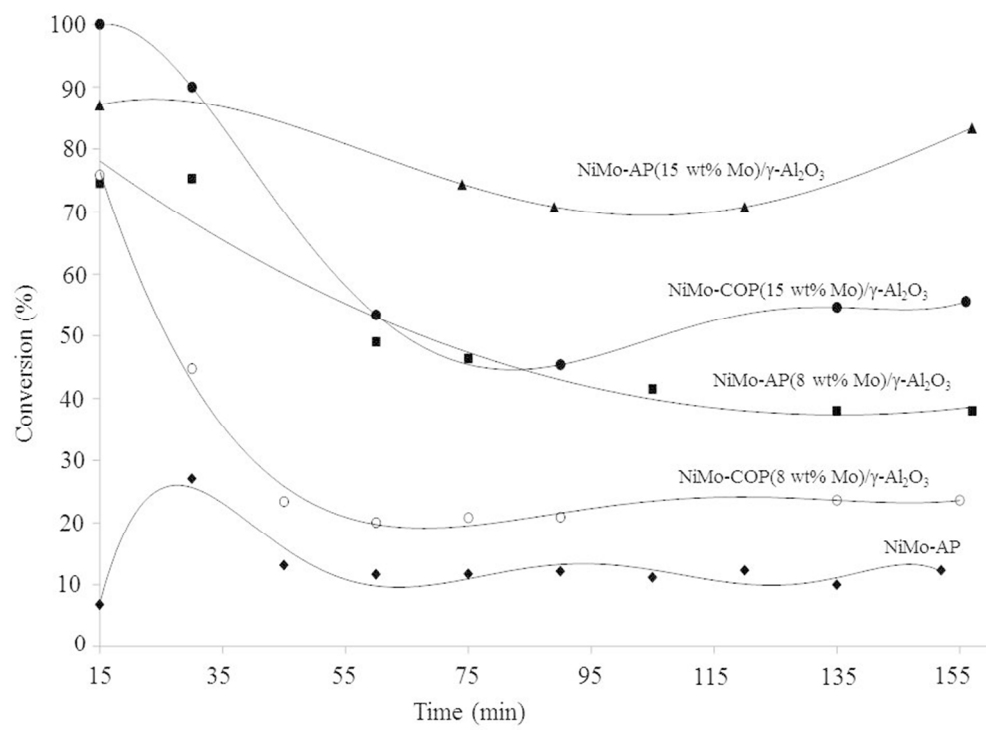
190x254mm (96 x 96 DPI)



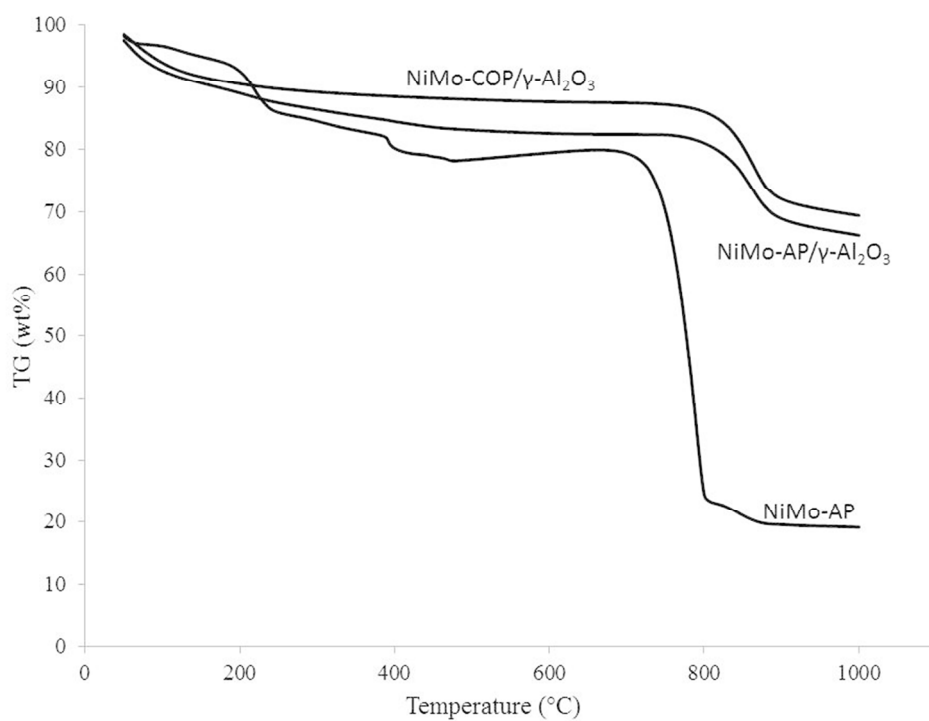
190x254mm (96 x 96 DPI)



254x190mm (96 x 96 DPI)



254x190mm (96 x 96 DPI)



254x190mm (96 x 96 DPI)

Table 1. Composition and textural properties in alumina supported Ni-Mo catalyst varying the type of precursor.

Solid	Nominal Composition			Experimental Composition			Specific Surface Area and Porous Characteristics.					Chemical Analysis (CHON-S)	
	Mo (wt%)	Ni (wt%)	Mo/Ni (atomic ratio)	Mo (wt%)	Ni (wt%)	Mo/Ni (atomic ratio)	A_{BET} (m ² /g)	V_T (cm ³ /g)	D_p (nm)	V_{meso} (cm ³ /g)	V_{mes}/V_T (%)	wt% C	wt% S
NiMo-AP	48.5	4.9	6	47.8	4.7	6	6	0.0038	2.5	0.0033	87	1,48	7,56
NiMo-AP (8 wt% Mo)/ γ -Al ₂ O ₃	8.0	0.8	6	7.00	0.7	6	387	0.419	4.3	0.339	81	0,82	4,26
NiMo-AP (15 wt% Mo)/ γ -Al ₂ O ₃	15	1.5	6	13.0	1.3	6	325	0.343	4.2	0.272	79	0,77	4,98
NiMo-COP (8 wt% Mo)/ γ -Al ₂ O ₃	8.0	0.8	6	7.00	0.6	7.5	283	0.267	3.8	0.208	78	0,83	4,22
NiMo-COP (15 wt% Mo)/ γ -Al ₂ O ₃	15	1.5	6	11.1	1.0	7	265	0.220	3.3	0.153	58	1,13	6,90

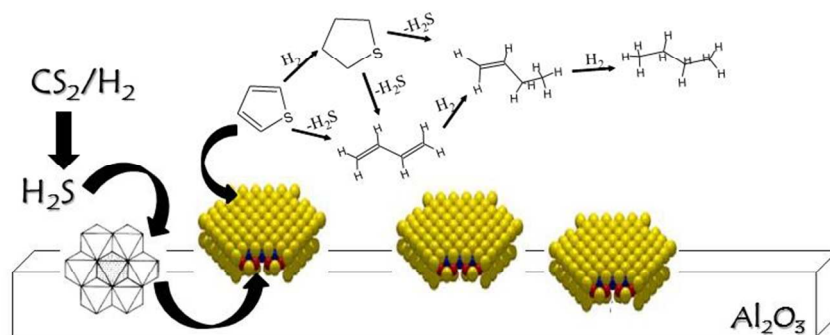
wt%: percentage by weight; A_{BET} : BET surface area; V_T : total volume of pores D_p : mean pore diameter; V_{meso} : mesopore volume; V_{mes}/V_T : fraction of the mesoporous to the total volume.

Table 2. Distribution of Mo and Ni oxidation states in alumina supported Ni-Mo catalyst using X-ray photoelectron spectroscopy and thiophene hydrodesulfurization activity.

Solid	Mo 3d _{5/2} -3d _{3/2}		Ni 2p _{3/2} -2p _{1/2}	Al 2p ^{-total}	atomic ratio			HDS Activity (mol Th/g Cat•min)x10 ⁶
	Mo ⁵⁺ eV (at%)	Mo ⁶⁺ eV (at%)	Ni ²⁺ eV (at%)	at%	Ni/Mo	Ni/Al	Mo/Al	
NiMo-AP (8 wt% Mo)/ γ -Al ₂ O ₃	230.9 (0.20)	232.5 (1.41)	-	28.74	-	-	0.06	126.8
NiMo-AP (15 wt% Mo)/ γ -Al ₂ O ₃	230.9 (0.83)	232.5 (1.84)	856.5 (0.34)	30.16	0.13	0.011	0.09	277.0
NiMo-COP (8 wt% Mo)/ γ -Al ₂ O ₃	-	232.5 (1.79)	-	35.14	-	-	0.05	80.1
NiMo-COP (15 wt% Mo)/ γ -Al ₂ O ₃	-	232.5 (4.61)	856.5 (1.17)	23.98	0.25	0.049	0.19	183.6

Table 3. Thiophene hydrodesulfurization conversion and selectivity at steady state of sulfided alumina-supported NiMo oxides: effect of wt % and precursor type.

precursor	Conversion (%)	Selectivity (%)		(Mo+Ni)/S
		butane	cis-butene	
NiMo-AP(8 wt% Mo)/ γ -Al ₂ O ₃	38.0	9,93	90,07	0,64
NiMo-AP(15 wt% Mo)/ γ -Al ₂ O ₃	83.4	12,75	87,25	1,01
NiMo-COP(8 wt% Mo)/ γ -Al ₂ O ₃	23.6	9,94	90,06	0,63
NiMo-COP(15 wt% Mo)/ γ -Al ₂ O ₃	55.6	11,52	88,48	0,62



The presulfided catalytic precursors from Anderson-type Heteropolyoxomolybdate
254x190mm (96 x 96 DPI)